A Survey on Reachable Set Techniques for Fault Recoverability Assessment

Martin Fauré, Jérôme Cieslak, David Henry, Anatole Verhaegen, Finn Ankersen

Available online at www.sciencedirect.com

ScienceDirect

IFAC PapersOnLine 55-6 (2022) 272–277

A Survey on Reachable Set Techniques for Fault Recoverability Assessment

Martin Fauré * **Jérôme Cieslak** * **David Henry** *
Anatole Verhaegen ** **Finn Ankersen** ***

* *IMS Lab. University of Bordeaux, CNRS, F-33405 Talence, France,*
{martin.faure,jerome.cieslak,david.henry}@ims-bordeaux.fr
** *Airbus Defence and Space SAS, 31402 Toulouse Cedex 4,*
anatole.verhaegen@airbus.com
*** *ESA / ESTEC, 2201 AZ Noordwijk, Netherlands,*
finn.ankersen@esa.int

Abstract: The development of any fault-tolerant control solution is based on the strong assumption that fault situations can be accommodated. This paper provides a survey of four reachable set techniques to assess the fault recoverability property for constrained linear time invariant (LTI) systems by means of ellipsoid, zonotope, polytope and support function representations. These techniques are next applied to an angular velocity spacecraft model. A discussion is finally made to assess the computational complexity for the four algorithms.

Keywords: Fault recoverability, reachable sets, ellipsoids, zonotopes, polytopes, support functions

1. INTRODUCTION

According to the studies by Tafazoli (2009); Henry et al. (2015), thruster failures in satellite and spacecraft account for more than 10 % of attitude and orbit control faults. In most situations, it can be shown that the consequences of faults could be avoided, or at least mitigated, by the use of Fault-Tolerant Control (FTC) solutions, see for instance Henry et al. (2015). Obviously, this promising feature is only true if the fault is labeled as recoverable (Staroswiecki and Berdjag, 2010), i.e. the ability of remaining plant resources permits to accommodate the considered fault situation and preserve the mission objectives. In this context, the development of tools able to characterize, from the first design phase, the plant fault tolerance properties are of great interest, especially to optimize the number and positioning of actuators on the satellite structure.

In spite of its practical importance, the assessment of plant fault-tolerant capabilities has received relatively little attention from the research community. The first works which have formulated this property in FTC community are Wu et al. (2000); Wu (2004) where a measure is given to quantify the level of redundancy of LTI models. A similar idea has been proposed in Yang et al. (2012) to switched system. More recently, it is proposed to use a controllability criterion in Yoshimura and Kojima (2018) to determine the optimal thruster location. In González-Contreras et al. (2009), an index based on reconfigurability is derived from an online computed controllability Gramian. Optimal piezo-electric actuator placement on plant structure is also done by optimizing a criteria based on controllability Gramian or energy consumption, see Frecker (2003). Unfortunately, the weakness of these techniques lies on the omission of actuator saturation, which can arise in case of faults. To overcome this issue, Chamseddine et al. (2015); Torres et al. (2017) and Sanjuan et al. (2019) propose to use attainable control set and one technique of reachable set to assess the fault reconfigurability property for a spacecraft and Unmanned Aerial Vehicles (UAV).

Based on these promising results, one contribution of this work is to provide a survey on four reachable set techniques and their computational complexity. Another contribution is to show how these methods can be used in the assessment of fault reconfigurability with a volume-based criterion.

This paper is organized as follows : section 2 introduces the reachability theory, section 3 describes the main set representation methods, section 4 is next devoted to computational aspects and section 5 presents the main methods with a simple satellite angular velocity model.

2. REACHABLE SETS

Reachable sets have been widely studied in control theory. Theoretical background is based on Hamilton-Jacobi (HJ) equations, leading to the level sets method (Mitchell, 2002). Other computation techniques involve the need of a set representation to allow set computations. Popular set representations are ellipsoids (Kurzhanski and Varaiya, 2010), zonotopes (Combastel, 2003), polytopes (Hwang et al., 2005) and support functions (Guernic and Girard, 2010). Having in mind this introduction, let the following time invariant dynamical system be considered

$$\dot{\boldsymbol{x}} = \boldsymbol{f}(\boldsymbol{x}, \boldsymbol{u}) \qquad \boldsymbol{x} \in \mathbb{R}^{n_x},\ \boldsymbol{u} \in \mathbb{R}^{n_u} \tag{1}$$

where $\boldsymbol{x}$ and $\boldsymbol{u}$ are the state and control input vectors respectively.

Given compact sets $\mathcal{X}_{t_0} \subset \mathbb{R}^{n_x}$ and $\mathcal{U}(t) \subset \mathbb{R}^{n_u}$, $\forall t \in [t_0, t_f]$, $t_0 < t_f$, the forward reachable set $\mathcal{R}_{t_f}(\mathcal{X}_{t_0})$ is the set of all states $\boldsymbol{x}(t_f)$ that can be reached at time t_f by the system (1) starting from time t_0, with $\boldsymbol{x}(t_0) \in \mathcal{X}_{t_0}$ and for all $\boldsymbol{u}(t) \in \mathcal{U}(t)$.

10.1016/j.ifacol.2022.07.141

The forward reachability tube $\mathcal{R}_{[t_0,t_f]}(\mathcal{X}_{t_0})$ is defined as the set of states attainable by the system (1) during the interval $[t_0, t_f]$:

$$\mathcal{R}_{[t_0,t_f]}(\mathcal{X}_{t_0}) = \bigcup_{t\in[t_0,t_f]} \mathcal{R}_t(\mathcal{X}_{t_0}) \tag{2}$$

By defining a value function $v(t,\ \boldsymbol{x})$ such that $\boldsymbol{x} \in \mathcal{R}_t(\mathcal{X}_{t_0}) \Leftrightarrow v(t,\ \boldsymbol{x}) \leq 0$, it can be shown using the dynamic programming principle that the forward reachability problem can be solved by the Hamilton-Jacobi-Bellman (HJB) partial derivative equation (PDE) (Kurzhanski and Varaiya, 2001)

$$\begin{cases} H(\boldsymbol{x},\ \boldsymbol{p}) & = \min\limits_{\boldsymbol{u}\in\mathcal{U}(t)} \left[\boldsymbol{p}^{\mathrm{T}}\ \boldsymbol{f}(\boldsymbol{x},\ \boldsymbol{u})\right] \\ 0 & = \dfrac{\partial v}{\partial t}(t,\ \boldsymbol{x}) + H\left(\boldsymbol{x},\ \dfrac{\partial v}{\partial x}(t,\ \boldsymbol{x})\right) \\ v(t_0,\ \boldsymbol{x}(t_0)) & \leq 0 \quad \forall \boldsymbol{x}(t_0) \in \mathcal{X}_{t_0} \end{cases} \tag{3}$$

where $H(\boldsymbol{x},\ \boldsymbol{p})$ is the Hamiltonian function. The equation (3) offers unfortunately no practical way to compute the reachable sets. In practice, we restrict the sets $\mathcal{X}$ and $\mathcal{U}$ to belong to a certain class, which allows the use of sets operators. In this framework, reachability computation of discrete time invariant systems

$$\boldsymbol{x}_{k+1} = \boldsymbol{A}_d\ \boldsymbol{x}_k + \boldsymbol{B}_d\ \boldsymbol{u}_k \tag{4}$$

is straightforward using linear mapping operator $(\boldsymbol{L}\cdot)$

$$\boldsymbol{L}\mathcal{S} = \{\boldsymbol{L}\boldsymbol{x} : \boldsymbol{x} \in \mathcal{S}\}$$

and Minkowski sum $(\cdot \oplus \cdot)$

$$\mathcal{S}_1 \oplus \mathcal{S}_2 = \{\boldsymbol{x} + \boldsymbol{y} : \boldsymbol{x} \in \mathcal{S}_1,\ \boldsymbol{y} \in \mathcal{S}_2\}$$

$\mathcal{S}$, $\mathcal{S}_1$ and $\mathcal{S}_2$ compact sets in $\mathbb{R}^n$, $\boldsymbol{L} \in \mathbb{R}^{p\times n}$, $p \in \mathbb{N}$:

$$\mathcal{X}_k = \boldsymbol{A}_d\ \mathcal{X}_{k-1} \oplus \boldsymbol{B}_d\ \mathcal{U}_{k-1} \tag{5}$$

Time discretization is mandatory for numerical computations, hence reachable sets for a continuous time invariant system

$$\dot{\boldsymbol{x}} = \boldsymbol{A}\ \boldsymbol{x} + \boldsymbol{B}\ \boldsymbol{u} \tag{6}$$

can not be computed exactly. Discretization with sampling rate T_s of LTI systems can be obtained with:

$$\boldsymbol{A}_d = \exp(\boldsymbol{A}T_s) \quad \boldsymbol{B}_d = \int_0^{T_s} \exp\left((T_s - s)\boldsymbol{A}\right)\boldsymbol{B}\mathrm{d}s$$

3. SET REPRESENTATIONS

Equation (5) is used to compute reachable sets for discrete-time linear systems when $\mathcal{X}_0$ and $\mathcal{U}_k$ belong to a set class that is closed under Minkowski sum and linear mapping. In this section, we present some popular set representations, emphasizing on some useful set operations for our application:

- Linear mapping $(\boldsymbol{L}\cdot)$ and Minkowski sum $(\cdot \oplus \cdot)$: these tools are necessary for computing the reachable set.
- Volume $(\mathrm{vol}(\cdot))$: used to compute the compensability criterion.
- Intersection $(\cdot \cap \cdot)$: can be used to compute the reachable set volume of union of sets. For example, given two sets $\mathcal{X}_1$ and $\mathcal{X}_2$, the volume of their union is $\mathrm{vol}\,\mathcal{X}_1 + \mathrm{vol}\,\mathcal{X}_2 - \mathrm{vol}\,(\mathcal{X}_1 \cap \mathcal{X}_2)$.

3.1 Ellipsoids

Ellipsoids of dimension n are affine transformations of an unit n-dimensional hyper-sphere

$$\mathcal{E} = \{\boldsymbol{c} + \boldsymbol{W}\boldsymbol{\xi} : \|\boldsymbol{\xi}\|_2 \leq 1\} \quad \boldsymbol{\xi} \in \mathbb{R}^n$$

where $\boldsymbol{c} \in \mathbb{R}^n$ is the center of the ellipsoid and $\boldsymbol{W} \in \mathbb{R}^{n\times n}$ is the transformation. When $\boldsymbol{W}$ is invertible, they can be represented by the equation

$$\begin{aligned} \mathcal{E} &= \left\{\boldsymbol{x} : (\boldsymbol{x} - \boldsymbol{c})^{\mathrm{T}}\boldsymbol{Q}^{-1}(\boldsymbol{x} - \boldsymbol{c}) \leq 1\right\} \quad \boldsymbol{x} \in \mathbb{R}^n \\ &= \{\boldsymbol{c},\ \boldsymbol{Q}\} \end{aligned}$$

with $\boldsymbol{Q} = \boldsymbol{W}\boldsymbol{W}^{\mathrm{T}}$ the shape matrix. To have a non-degenerate ellipsoid, $\boldsymbol{Q}$ must be definite positive $\boldsymbol{Q} \succ 0$. Ellipsoids are closed under linear mapping:

$$\boldsymbol{L}\mathcal{E} = \left\{\boldsymbol{L}\boldsymbol{c},\ \boldsymbol{L}\boldsymbol{Q}\boldsymbol{L}^{\mathrm{T}}\right\}$$

However, ellipsoids are not closed under Minkowski sum and intersection. In order to perform reachability computations, a minimum volume outer ellipsoidal (MVOE) approximation of the Minkowski sum can be performed. This approximation can be constructed with the algorithm from Halder (2018) presented here:

Proposition 1. (MVOE approximation (Halder, 2018)).

$$\begin{aligned} \{\boldsymbol{c},\ \boldsymbol{Q}\} &= \{\boldsymbol{c}_1,\ \boldsymbol{Q}_1\} \oplus \{\boldsymbol{c}_2,\ \boldsymbol{Q}_2\} \\ \boldsymbol{c} &= \boldsymbol{c}_1 + \boldsymbol{c}_2 \\ \boldsymbol{Q} &= \left(1 + \frac{1}{\beta}\right)\boldsymbol{Q}_1 + (1+\beta)\,\boldsymbol{Q}_2 \end{aligned}$$

The new shape matrix $\boldsymbol{Q}$ is parametrized by a scalar β. Its optimal value is found using the following recursive equation which is always convergent

$$\beta_{k+1} = \sqrt{\frac{\sum_{i=1}^{n} \frac{1}{1+\beta_k\lambda_i}}{\sum_{i=1}^{n} \frac{\lambda_i}{1+\beta_k\lambda_i}}}$$

where n is the dimension of the ellipsoid, and λ_i, $i = 1, \ldots, n$ are the eigenvalues of $\boldsymbol{Q}_1^{-1}\boldsymbol{Q}_2$.

Volume of an ellipsoid is computed with the formula

$$\mathrm{vol}(\mathcal{E}) = \frac{\pi^{\frac{n}{2}}}{\Gamma\left(\frac{n}{2}+1\right)}\sqrt{\det \boldsymbol{Q}} \tag{7}$$

where Γ is the standard gamma function (Halder, 2018).

3.2 Polytopes

Polytopes are bounded convex polyhedron which are the intersection of a finite number of half-spaces. A polytope $\mathcal{P}$ in dimension n has two equivalent representations:

- $\mathcal{H}$-representation where the polytope is represented by its m half-spaces using linear inequalities:
$$\mathcal{P} = \{\boldsymbol{x} : \boldsymbol{H}\boldsymbol{x} \leq \boldsymbol{b}\} \quad \boldsymbol{x} \in \mathbb{R}^n \quad \boldsymbol{H} \in \mathbb{R}^{m\times n}$$
- $\mathcal{V}$-representation where the polytope is represented by the convex hull of its p vertices $\boldsymbol{V}$:
$$\mathcal{P} = \mathrm{conv}(\boldsymbol{V}) \qquad \boldsymbol{V} \in \mathbb{R}^{p\times n}$$

Finding the $\mathcal{V}$-representation of a polytope given the $\mathcal{H}$-representation is called the vertex enumeration problem, and finding the $\mathcal{H}$-representation with the $\mathcal{V}$-representation is the facet enumeration problem. By geometric duality, these two problems are equivalent. Polytopes are closed under linear mapping, Minkowski sum and intersection. Linear mapping and intersection can be computed easily in $\mathcal{H}$-representation:

$$\boldsymbol{L}\mathcal{P} = \left\{\boldsymbol{x} : \boldsymbol{H}\boldsymbol{L}^{-1}\boldsymbol{x} \leq \boldsymbol{b}\right\} \tag{8}$$

$$\mathcal{P}_1 \cap \mathcal{P}_2 = \left\{\boldsymbol{x} : \begin{bmatrix}\boldsymbol{H}_1\\ \boldsymbol{H}_2\end{bmatrix}\boldsymbol{x} \leq \begin{bmatrix}\boldsymbol{b}_2\\ \boldsymbol{b}_2\end{bmatrix}\right\}$$

Minkowski sum is harder to compute and usually require two steps (Kvasnica, 2005):

$$\mathcal{P}_1 \oplus \mathcal{P}_2 = \text{proj}\left\{\boldsymbol{x} \in \mathbb{R}^n : \begin{bmatrix}\boldsymbol{H}_2 & -\boldsymbol{H}_2\\ \boldsymbol{0} & \boldsymbol{H}_1\end{bmatrix}\begin{bmatrix}\boldsymbol{x}\\ \boldsymbol{x}_1\end{bmatrix} \leq \begin{bmatrix}\boldsymbol{b}_2\\ \boldsymbol{b}_1\end{bmatrix}\right\} \tag{9}$$

proj is the projection along the dimensions of $\boldsymbol{x}$. This projection can easily be done in $\mathcal{V}$-representation:

$$\text{proj}\,\mathcal{P} = \text{conv}\left(\boldsymbol{V}_{1,\dots,n}\right) \tag{10}$$

The volume of a polytope can be calculated exactly from both of the representations (Lawrence, 1991).

3.3 Zonotopes

Zonotopes are symmetric polytopes. A zonotope $\mathcal{Z}$ of dimension n with p generators can be formed by the affine transformation of a unit hypercube (Scott et al., 2016)

$$\begin{aligned}\mathcal{Z} &= \{\boldsymbol{c} + \boldsymbol{G}\boldsymbol{\xi} : \|\boldsymbol{\xi}\|_\infty \leq 1\} \quad \boldsymbol{\xi} \in \mathbb{R}^p\\ &= \{\boldsymbol{c},\ \boldsymbol{G}\}\end{aligned}$$

where $\boldsymbol{c} \in \mathbb{R}^n$ is the center of the zonotope and $\boldsymbol{G} \in \mathbb{R}^{n\times p}$ is the generator matrix. Equivalently, it is also the Minkowski sum of the generators

$$\mathcal{Z} = \boldsymbol{c} + \bigoplus_{i=1}^{p} \boldsymbol{G}^i$$

where $\boldsymbol{G}^i$ represents the ith generator (i.e. the ith column of $\boldsymbol{G}$). Zonotopes are closed under linear mapping and Minkowski sum:

$$\begin{aligned}\boldsymbol{L}\mathcal{Z} &= \{\boldsymbol{L}\boldsymbol{c},\ \boldsymbol{L}\boldsymbol{G}\}\\ \mathcal{Z}_1 \oplus \mathcal{Z}_2 &= \left\{\boldsymbol{c}_1 + \boldsymbol{c}_2,\ \begin{bmatrix}\boldsymbol{G}_1 & \boldsymbol{G}_2\end{bmatrix}\right\}\end{aligned}$$

However, zonotopes are not closed under intersection. The volume of a zonotope is

$$\text{vol}(\mathcal{Z}) = 2^n \sum_{1\leq j_1<\dots<j_n\leq p} \left|\det\left(\boldsymbol{G}^{j_1,\dots,j_n}\right)\right|$$

$j_1, \dots, j_n$ represents n columns chosen among the p columns of $\boldsymbol{G}$. The sum is performed over the $\binom{p}{n}$ combinations (Gover and Krikorian, 2010).

When using zonotopes for reachability computations, the number of generators of the computed zonotope increases steadily because of the Minkowski sum. To limit this growth, several zonotopes reduction techniques have been developed, see Combastel (2003); Scott et al. (2016).

3.4 Support functions

Support functions are used to represent convex sets. A support function $\rho(\boldsymbol{l})$ representing the convex set $\mathcal{S}$ in dimension n is defined as Girard and Guernic (2008):

$$\begin{aligned}\rho\ :\ &\mathbb{R}^n \to \mathbb{R}\\ &\boldsymbol{l} \mapsto \max_{\boldsymbol{x}\in\mathcal{S}} \boldsymbol{l}^{\mathrm{T}}\boldsymbol{x}\end{aligned}$$

Several convex sets can be easily represented as support functions:

- Ellipsoids $\mathcal{E} = \{\boldsymbol{c},\ \boldsymbol{Q}\}$:
$$\rho_{\mathcal{E}}(\boldsymbol{l}) = \boldsymbol{l}^{\mathrm{T}}\boldsymbol{c} + \sqrt{\boldsymbol{l}^{\mathrm{T}}\boldsymbol{Q}\boldsymbol{l}}$$
- Zonotopes $\mathcal{Z} = \{\boldsymbol{c},\ \boldsymbol{G}\}$:
$$\rho_{\mathcal{Z}}(\boldsymbol{l}) = \boldsymbol{l}^{\mathrm{T}}\boldsymbol{c} + \sum_{i=1}^{p}\left|\boldsymbol{l}^{\mathrm{T}}\boldsymbol{G}^i\right|$$
- Polytopes in $\mathcal{H}$-representation $\mathcal{P} = \{\boldsymbol{x} : \boldsymbol{H}\boldsymbol{x} \leq \boldsymbol{b}\}$:
$$\rho_{\mathcal{P}}(\boldsymbol{l}) = \max_{\boldsymbol{x}} \boldsymbol{l}^{\mathrm{T}}\boldsymbol{x} \qquad \text{under constraints } \boldsymbol{H}\boldsymbol{x} \leq \boldsymbol{b}$$
- Polytopes in $\mathcal{V}$-representation $\mathcal{P} = \text{conv}(\boldsymbol{V})$:
$$\rho_{\mathcal{P}}(\boldsymbol{l}) = \max\left(\boldsymbol{V}\boldsymbol{l}\right)$$
where $\boldsymbol{V}$ is the matrix of the vertices, and max selects the maximum element in the column vector.

Polytopes can be seen as "sampled" support functions. With a finite number of direction vectors $\left\{\boldsymbol{l}^1, \dots, \boldsymbol{l}^p\right\}$, it follows that

$$\left\{\boldsymbol{x} : \begin{bmatrix}\boldsymbol{l}^1 & \dots & \boldsymbol{l}^p\end{bmatrix}^{\mathrm{T}}\boldsymbol{x} \leq \begin{bmatrix}\rho(\boldsymbol{l}^1)\\ \vdots\\ \rho(\boldsymbol{l}^p)\end{bmatrix}\right\}$$

is a polytope that over approximates the support function $\rho(\boldsymbol{l})$. Support functions are closed under linear mapping, Minkowski sum and intersection:

$$\begin{aligned}\boldsymbol{L}\rho(\boldsymbol{l}) &= \rho(\boldsymbol{L}^{\mathrm{T}}\boldsymbol{l})\\ \rho_{\mathcal{S}_1\oplus\mathcal{S}_2}(\boldsymbol{l}) &= \rho_{\mathcal{S}_1}(\boldsymbol{l}) + \rho_{\mathcal{S}_2}(\boldsymbol{l})\end{aligned}$$

Intersection of support functions can be computed with:

$$\rho_{\mathcal{S}_1\cap\mathcal{S}_2}(\boldsymbol{l}) = \min\left(\rho_{\mathcal{S}_1}(\boldsymbol{l}),\ \rho_{\mathcal{S}_2}(\boldsymbol{l})\right) \tag{11}$$

Unfortunately, the equation (11) does not belong to the support function class due to redundancy. However, an exact solution can be computed using the polar duality $*$: $\rho^*(\boldsymbol{l}) = \frac{1}{\rho(\boldsymbol{l})}$ (Ghosh and Kumar, 1998):

$$\rho_{\mathcal{S}_1\cap\mathcal{S}_2}(\boldsymbol{l}) = \left(\max\left(\rho^*_{\mathcal{S}_1}(\boldsymbol{l}),\ \rho^*_{\mathcal{S}_2}(\boldsymbol{l})\right)\right)^*$$

Volume of a support function can be computed by sampling it and using a $\mathcal{H}$-representation method.

4. COMPUTATIONAL ASPECTS

In this section, it is firstly proposed to assess the algorithmic computational complexity for the aforementioned set operations to evaluate a volume of reachable sets. The second subsection will introduce in a general context the proposed fault recoverability criterion.

4.1 Computational issues

Table 1 summarize the algorithmic computational complexity for the set operations. It is assumed that any operation over a scalar is $O(1)$ (.i.e done in constant time), and $n \times n$ matrix multiplication is $O\left(n^3\right)$. Any matrix concatenation is $O(1)$. n denotes the dimension of the set, p the number of elements (i.e. the numbers of half-spaces for $\mathcal{H}$-representation, of vertices for $\mathcal{V}$-representation, of generators for zonotope and the number of direction vectors for support functions). S denotes the computational complexity of evaluation of $\rho(\boldsymbol{l})$ where $\boldsymbol{l}$ is a direction vector.

Linear mapping for $\mathcal{H}$-representation is computed with equation (8). Minkowski sum for polytope is computed

Table 1. Computational complexity $O(\cdot)$ for set operations

Rep	$\boldsymbol{L}\cdot$	$\cdot \oplus \cdot$	$\cdot \cap \cdot$	vol$(\cdot)$
Ellipsoid	$2n^3$	-	-	n^3
$\mathcal{H}$-rep	pn^2+n^3	$(p_1+p_2)^n$	1	p^n
$\mathcal{V}$-rep	pn^2	$(p_1+p_2)^n$	$(p_1+p_2)^{\frac{n}{2}}$	$p^{\frac{n}{2}}$
Zonotope	pn^2	1	-	$\binom{p}{n}n^3$
Supp. func.	pn^2+pS	$p+2pS$	$4p+2pS$	p^n

with equations (9)-(10). Facets or vertices enumeration problems are computed with the software cdd (Fukuda, 2019) or toolbox MPT3 (Herceg et al., 2013), computational complexity is assumed to be $O\left(p^{\frac{n}{2}}\right)$. Volume for $\mathcal{H}$-representation polytope is computed with the revisited Lasserre algorithm, implemented in VINCI (Büeler and Enge, 2003) software.

4.2 Fault recoverability criterion

The fault recoverability criterion J is computed as the relative difference between the volumes of the fault-free reachable set $\mathcal{R}$ and the faulty reachable set $\mathcal{R}_f$ at time t_f (Chamseddine et al., 2015; Torres et al., 2017). By this definition, the (normalized) criterion is defined by:

$$J = \frac{\operatorname{vol}\mathcal{R} - \operatorname{vol}\mathcal{R}_f}{\operatorname{vol}\mathcal{R}} \tag{12}$$

5. NUMERICAL ILLUSTRATION

The introduced reachable set methods are now tested on a standard satellite angular velocity model. The first objective is to select the most suitable one in terms of computational complexity and conservatism to integrate it in the fault recoverability assessment. The selected method is finally applied to faulty satellite to highlight the lost domains in fault situations.

5.1 Angular velocity model of a satellite

Satellite rotational motion can be modeled in the body-fixed frame of the satellite R_b (whose origin is the center of mass of the satellite) using second law of Euler

$$\dot{\boldsymbol{\omega}} = \boldsymbol{J}^{-1}\sum_k \boldsymbol{T}_k - \boldsymbol{J}^{-1}\boldsymbol{\omega}\times\boldsymbol{J}\boldsymbol{\omega} \tag{13}$$

where $\boldsymbol{\omega} = [p\ q\ r]^{\mathrm{T}}$ is the angular velocity vector, $\boldsymbol{J}\in\mathbb{R}^{3\times3}$ is the inertia matrix, $\sum_k \boldsymbol{T}_k \in \mathbb{R}^3$ is the sum of externally applied torques and $\times$ denotes the cross product. The satellite uses twelve thrusters, which are normalized to take inputs between 0 (thruster fully closed) and 1 (thruster fully open), collected in the command vector $\boldsymbol{u}$. In this study case, disturbances are not considered. Hence, thrusters are the only source of torques

$$\sum_k \boldsymbol{T}_k = \boldsymbol{M}_{thr}\boldsymbol{u} \tag{14}$$

with $\boldsymbol{M}_{thr} \in \mathbb{R}^{3\times12}$ denotes the thruster configuration matrix which projects the thrusters' space in the moments' space. The non-linear obtained model can be put in state-space form then linearized around the equilibrium point

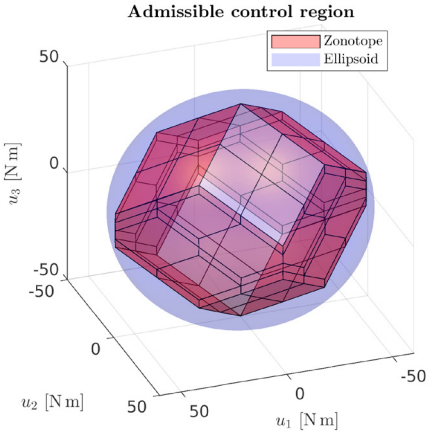

Fig. 1. Exact zonotope command set, and its MVOE enclosure

$\boldsymbol{\omega} = \boldsymbol{0}$ and discretized with $T_s = 0.1\,\mathrm{s}$, which yields to the following discrete LTI model:

$$\boldsymbol{x}_{k+1} = \mathbb{I}_3\boldsymbol{x}_k + \boldsymbol{B}_d\boldsymbol{M}_{thr}\boldsymbol{u}_k \tag{15}$$

with $\mathbb{I}_n$ the identity matrix of dimension n.

5.2 Computation of reachability set volume in fault-free case

The initial state $\boldsymbol{x}_0$ is fixed at the origin $\boldsymbol{x}_0 = \boldsymbol{0}$. The control input $\boldsymbol{u}$ can be anywhere inside the possible control set which is the 12-hypercube. By definition, the command set can thus be a zonotope $\mathcal{U} = \frac{1}{2}\boldsymbol{M}_{thr}\{\boldsymbol{1}_{12}, \mathbb{I}_{12}\}$, where $\boldsymbol{1}_{12}$ is a twelve dimensional column vector of ones. Note that thruster inputs are normalized to be between 0 and 1, not -1 and 1, hence the factor $\frac{1}{2}$. This zonotope is plotted on figure 1. It is proposed now to compute the reachable set for the next five steps, i.e the simulation is run for 0.5 s.

Ellipsoid The command set is transformed into an ellipsoid using a minimum volume outer approximation. The center $\boldsymbol{c}$ of the ellipsoid is the same as the center of the zonotope ; the shape matrix $\boldsymbol{Q}$ is found with the following optimization program which uses the $\mathcal{V}$-representation of $\mathcal{U}$ (Gotoh and Konno, 2006)

$$\boldsymbol{Q} = \arg\min_{\boldsymbol{Q}} \log\left(\det\boldsymbol{Q}\right)$$
$$\text{under constraints} \begin{cases} (\boldsymbol{v}-\boldsymbol{c})^{\mathrm{T}}\boldsymbol{Q}^{-1}(\boldsymbol{v}-\boldsymbol{c}) & \forall \boldsymbol{v}\in\boldsymbol{V}_{\mathcal{U}} \\ \boldsymbol{Q}\succ 0 \end{cases}$$

with $\boldsymbol{V}_{\mathcal{U}}$ that corresponds to the vertices of $\mathcal{U}$.

The volume computed with equation (7) is reported in table 2.

Polytope $\mathcal{H}$-representation of the command set can be obtained using the algorithm presented in Althoff et al. (2010). Based on the model (15), the results of polytope computations are given in table 2. From these results, it can be seen that there is some numerical problem leading to an overestimated set volume.

Polytope $\boldsymbol{B_d}$ To overcome the numerical computation issue, let the model

$$\boldsymbol{x}_{k+1} = \boldsymbol{A}_d\boldsymbol{x}_k + \mathcal{U}_{\boldsymbol{B}_d}$$

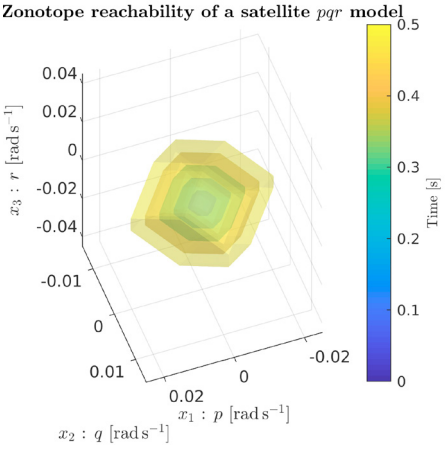

Fig. 2. Zonotopes reachability of the satellite *pqr* model

be considered. $\mathcal{U}_{\boldsymbol{B}_d}$ is the command polytope obtained from the zonotope $\frac{1}{2}\boldsymbol{B}_d\boldsymbol{M}_{thr}\{\mathbf{1}_{12}, \mathbb{I}_{12}\}$. Polytope simulations are implemented using the MPT3 Toolbox (Herceg et al., 2013). Results are reported in table 2.

Zonotope The command set being a zonotope, computation is straightforward using model (15) and equation (5).

Support function 400 vectors are chosen to linearly span all the directions. The command support function is then computed by over-approximating the $\mathcal{H}$-representation of the command polytope set. The results are inserted in table 2.

Support function with integrator model The model (15) is an integrator. To take advantage of this feature, proposition 2 is considered to exactly compute the reachable set.

Proposition 2. Given $\mathcal{X}_0 = \mathbf{0}$ the initial state and $\mathcal{U} = \{\boldsymbol{x} : \boldsymbol{H}_{\mathcal{U}}\boldsymbol{x} \leq \boldsymbol{b}_{\mathcal{U}}\} \quad \boldsymbol{x} \in \mathbb{R}^{n_u}$ the command set, the support function reachable sets with an integrator model can be computed exactly with the equation

$$\rho_{\mathcal{X}_k}(\boldsymbol{H}_{\mathcal{U}}) = \rho_{\mathcal{X}_{k-1}}(\boldsymbol{H}_{\mathcal{U}}) + \rho_{\mathcal{U}}(\boldsymbol{H}_{\mathcal{U}})$$

Results are reported in table 2.

Selection of the most efficient reachable set tool Table 2 summaries the results of the simulation. The polytope $\boldsymbol{B}_d$, zonotope and support function integrator are expected to give the exact solution. The other methods give conservative approximations. In regard to the desired properties, zonotope and support function (integrator) give the best trade-offs. Zonotopes allow fast and exact computations. However, they can only represent symmetric convex sets and intersection computations are not possible, which can further complicate their use with more complex sets for volume computation. On the other hand, support function integrator are flexible tool and can represent any convex set. In this context, the intersection computation can easily be extended to non-convex sets for volume computation. If support functions only provide over-approximations, the tightness is completely tunable through the choice of the direction vectors. Based on this analysis, the volume involved in the fault recoverability criterion will be obtained by support function for integrator system.

Table 2. Simulation results for the different reachability methods

Method	Set volume	Simulation time
Polytopes	2.8970×10^{-5}	3 m
Ellipsoids	2.3247×10^{-5}	5.4440×10^{-3} s
Support functions	1.4514×10^{-5}	5.9447 s
Polytopes $\boldsymbol{B}_d$	1.2800×10^{-5}	7.1847×10^{-1} s
S.F. Integrator	1.2614×10^{-5}	1.8200×10^{-3} s
Zonotopes	1.2562×10^{-5}	8.5230×10^{-3} s

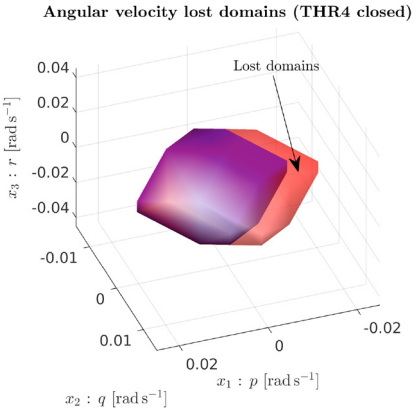

Fig. 3. Reachable set at time t_f computed with support functions in the fault-free case (red), and with thruster 4 closed (blue)

5.3 Computation of fault recoverability criterion

We now consider the case of one thruster failure in model (15). The faults considered are: the thruster is blocked in closed position, its command is always 0; or the thruster is blocked in open position, its command is always 1. We make the assumption that two faults cannot occur simultaneously. The faulty command set can still be represented by a zonotope

$$\mathcal{U} = \frac{1}{2}\boldsymbol{B}_d\boldsymbol{M}_{thr}\{\boldsymbol{c}, \boldsymbol{G}\}$$

with $\boldsymbol{c}$ a twelve dimensional column vector of ones except on the row of the faulty thruster which is zero when the thruster is closed and two when the thruster is open. $\boldsymbol{G}$ is a twelve dimensional diagonal matrix of ones except on the index of the faulty thruster which is zero (for both faults).

The simulations are run using support functions and the direction vectors are chosen to be the normal of the facets of $\mathcal{U}$. Since the model (15) is an integrator, this results in exact computations. The obtained values of the criteria J are presented in table 3. These results are the same as those obtained in Torres et al. (2017). Figure 3 shows the difference between the fault-free case and the case with thruster 4 closed. Results show that the loss of control authority is the same for opened and closed faults, which is coherent given that the corresponding command zonotopes have the same generator matrix.

6. CONCLUSION / FUTURE WORKS

In this paper, an overview of four reachable set computation methods are firstly presented. Among the tested methods,

Table 3. Loss of control authority (value of J) in % for all considered faults

Fault	THR1	THR2	THR3	THR4	THR5	THR6	THR7	THR8	THR9	THR10	THR11	THR12
Closed	34.15	34.25	6.98	34.14	33.77	6.71	34.25	34.15	6.98	33.77	34.14	6.71
Opened	34.15	34.25	6.98	34.14	33.77	6.71	34.25	34.15	6.98	33.77	34.14	6.71

two seems particularly suitable: zonotopes with the advantages of fast and exact computation, but the drawbacks that zonotopes can only represent symmetric convex sets ; and support functions which are very flexible and quite fast to compute, even if results are often over-approximations. The computed reachable set can then be used to form a fault recoverability criterion. Relative difference between the nominal case and thruster failures cases can be used to quantify the loss of control authority. In future works, the test of the inclusion of the reference trajectory in the faulty reachability tube will be used to determine if a fault is recoverable. In addition, it will be welcome to provide tools able to take into account the effect of disturbances and model parametric uncertainties. This is the topic of our future works.

REFERENCES

Althoff, M., Stursberg, O., and Buss, M. (2010). Computing reachable sets of hybrid systems using a combination of zonotopes and polytopes. *Nonlinear Analysis: Hybrid Systems*.

Büeler, B. and Enge, A. (2003). VINCI webpage.

Chamseddine, A., Join, C., and Theilliol, D. (2015). Trajectory planning/re-planning for satellite systems in rendezvous mission in the presence of actuator faults based on attainable efforts analysis. *International Journal of Systems Science 46:4*.

Combastel, C. (2003). A state bounding observer based on zonotopes. In *European Control Conference*.

Frecker, M.I. (2003). Recent advances in optimization of smart structures and actuators. *Journal of Intelligent Material Systems and Structures Vol. 14*.

Fukuda, K. (2019). `cddlib` repository. `https://github.com/cddlib/cddlib`.

Ghosh, P.K. and Kumar, K.V. (1998). Support function representation of convex bodies, its application in geometric computing, and some related representations. *Computer Vision and Image Understanding Vol. 72, No. 3*.

Girard, A. and Guernic, C.L. (2008). Efficient reachability analysis for linear systems using support functions. In *The International Federation of Automatic Control*.

González-Contreras, B., Theilliol, D., and Sauter, D. (2009). On-line reconfigurability evaluation for actuator faults using input/output data. In *7th IFAC Symposium on Fault Detection, Supervision and Safety of Technical Processes*.

Gotoh, Y.Y. and Konno, H. (2006). Minimal ellipsoid circumscribing a polytope defined by a system of linear inequalities. *Journal of Global Optimization*.

Gover, E. and Krikorian, N. (2010). Determinants and the volumes of parallelotopes and zonotopes. *Linear Algebra and its Applications 433*, 28–40.

Guernic, C.L. and Girard, A. (2010). Reachability analysis of linear systems using support functions. *Nonlinear Analysis: Hybrid Systems 4*.

Halder, A. (2018). On the parameterized computation of minimum volume outer ellipsoid of minkowski sum of ellipsoids. In *IEEE Conference on Decision and Control*.

Henry, D., Peuvédic, C.L., Strippoli, L., and Ankersen, F. (2015). Robust model-based fault diagnosis of thruster faults in spacecraft. In *The International Federation of Automatic Control*.

Herceg, M., Kvasnica, M., Jones, C., and Morari, M. (2013). Multi-parametric toolbox 3.0. In *Proc. of the European Control Conference*.

Hwang, I., Stipanović, D.M., and Tomlin, C.J. (2005). Polytopic approximations of reachable sets applied to linear dynamic games and a class of nonlinear systems. In B. Boston (ed.), *Advances in Control, Communication Networks, and Transportation Systems*.

Kurzhanski, A.B. and Varaiya, P. (2001). Dynamic optimization for reachability problems. In P.P. Corporation (ed.), *Journal of optimization theory and applications*, volume 108, 227–251.

Kurzhanski, A.B. and Varaiya, P. (2010). *Dynamics and Control of Trajectory Tubes*. Birkhäuser.

Kvasnica, M. (2005). Minkowski addition of convex polytopes.

Lawrence, J. (1991). Polytope volume computation. *Mathematics Of Computation*.

Mitchell, I.M. (2002). Application of level set methods to control and reachability problems in continuous and hybrid systems.

Sanjuan, A., Nejjari, F., and Sarrate, R. (2019). Reconfigurability analysis of multirotor uavs under actuator faults. In *4th Conference on Control and Fault Tolerant Systems*.

Scott, J.K., Raimondo, D.M., Marseglia, G.R., and Braatz, R.D. (2016). Constrained zonotopes: A new tool for set-based estimation and fault detection. *Automatica*.

Staroswiecki, M. and Berdjag, D. (2010). A general fault tolerant linear quadratic control strategy under actuator outages. *International Journal of Systems Science 41:8*.

Tafazoli, M. (2009). A study of on-orbit spacecraft failures. *Acta Astronautica 64*.

Torres, J.Z., Cieslak, J., Henry, D., and Dávila, J. (2017). Fault compensability criteria with application to a rendezvous mission around mars. In *14th International Workshop on Advenced Control and Diagnosis*.

Wu, N.E. (2004). Coverage in fault-tolerant control. *Automatica 40:4*.

Wu, N.E., Zhou, K., and Salomon, G. (2000). Control reconfigurability of linear time-invariant systems. *Automatica 36:11*.

Yang, H., Jiang, B., and Staroswiecki, M. (2012). Fault recoverability analysis of switched systems. *International Journal of Systems Science 43:3*.

Yoshimura, Y. and Kojima, H. (2018). Optimization of fault-tolerant thruster configurations for satellite control. *Advances in Space Research 61*.